Supporting Information

Few-layered Tungsten Selenide as Cocatalyst for Visible-light-driven Photocatalytic Production of Hydrogen Peroxide for Bacterial Inactivation

Wanjun Wang, Wenquan Gu, Guiying Li, Haojing Xie, Po Keung Wong, Taicheng An*

Guangdong Key Laboratory of Environmental Catalysis and Health Risk Control, Guangzhou Key Laboratory Environmental Catalysis and Pollution Control, School of Environmental Science and Engineering, Institute of Environmental Health and Pollution Control, Guangdong University of Technology, Guangzhou 510006, China.

Corresponding author

Tel: +86 20 3932 2298, Fax: +86 20 3932 2298, E-mail: antc99@gdut.edu.cn (T.C. An);

Pages: 14

Contents: Environmental details;

Nine Figures (Figure S1-S9)

One Table (Table S1)

1. Fabrication of WSe_2 nanosheets

WSe_2 nanosheets was prepared by one-step solvothermal method.[1, 2] Briefly, 200 mg of $NaBH_4$, 640 mg of Se powder, and 1.32 g of $Na_2WO_4 \cdot 2H_2O$ were weighed and dissolved in 60 mL Dimethyl Formamide (DMF) solution. Then, the obtained mixtures were vigorously stirred for 3 h. Subsequently, the mixtures were transferred into a 100 mL autoclave, which was maintained at 240 ^oC in an electric furnace for 24 h. After cooling naturally, the product was collected by centrifuged. Subsequently, washed several times with DI water and absolute ethanol, and dried at 60 ^oC under vacuum for 24 h. The composite was annealed at 300 ^oC for 5 h under Ar atmosphere to obtain the final product.

2. Characterization of materials

Crystallographic structures of the as-prepared materials were recorded X-ray diffractometer (XRD) (Cu Kα, D/max-Ultima IV). The structure of composite photocatalyst was characterized by a Fourier transform infrared spectrometer (FT-IR, Nicolet is10). UV−vis absorption spectra was obtained by an UV–vis Cary 100 spectrophotometer equipped with a labsphere diffuse reflectance accessory (Agilent, USA). Morphologies and microstructures of the products were examined by scanning electron microscopy (SEM) (SU8220, Hitach, Japan) and transmission electron microscopy (TEM) (FE-HRTEM, Talos F200s, FEI Company). High-angle annular dark field (HAADF) and energy dispersive X-ray spectroscopy (EDS) were completed on transmission electron microscopy (TEM) too. The X-ray photoelectron spectroscopy (XPS) was used to analysis surface electronic states (Escalab 250Xi, Thermo Fisher Scientific). All binding energies were calibrated using contaminant carbon (C1s = 284.8

eV). Photoluminescence spectra (PL) and time-resolved PL spectra of the samples were obtained at room temperature excited by incident light of 365 nm using a fluorescence spectrometer (Edinburgh FLS1000). The time-resolved fluorescence decay was fitted by the following equation (1):

$$I(t) = A_1 \exp(-t/\tau_1) + A_2 \exp(-t/\tau_2) \quad (1)$$

where τ_1 and τ_2 represent the fluorescence lifetime, A_1 and A_2 represent the relative amplitudes. The fluorescence lifetime τ_1 (short lifetime) was assigned to the non-radiative recombination of the photo-induced electrons with the surface defects; the fluorescence lifetime τ_2 (long lifetime) was derived from the bandgap charge-carriers recombination. The average fluorescence lifetimes (τ_{Avg}) were calculated according to the equation (2):[3]

$$\tau_{Avg} = \frac{A_1\tau_1^2 + A_2\tau_2^2}{A_1\tau_1 + A_2\tau_2} \quad (2)$$

3. Photoelectrochemical measurements

Electrochemical impedance spectroscopy (EIS) and photocurrent tests were conducted on an electrochemical workstation (CHI 650E, Shanghai Chenhua Instruments, China) with a standard three-electrode cell, using a Pt plate and a saturated Ag/AgCl electrode as counter electrode and reference electrode, respectively The working electrodes were prepared on the fluorine doped tin oxide (FTO) glass. The electrolyte used was 0.1 M Na_2SO_4 aqueous solution. 7 mg catalysis was mixed with 0.25 mL ethanol and 10 μL nafion solution by ultrasonicating for 30 min. The mixture was loaded on FTO glass and dry at 60 ^{o}C under atmospheric air. A 300 W Xe lamp with a 420 nm cut-off filter acted as the light source in the tests. Photocurrent measurements were recorded with a bias potential of 0.1 V. The EIS examinations were

conducted across the frequency range of 10^{-2} Hz - 10^{5} Hz on applied voltage of 0 V with an AC perturbation signal of 5 mV. The Mott-Schottky measurement was performed at frequency of 500 Hz and 1000 Hz.

Rotating disc electrode (RDE, Pine Co. Ltd) tests were employing to investigate the number of electron transfer for O_2 reduction. 2 mg of catalysts were dispersed in 1 mL of 1% nafion. After ultrasonication for 30 min, 10 μL of homogenous ink was adhered onto glassy carbon electrodes (GCE) as the working electrode. The Linear sweep voltammetry (LSV, 50mV/s scan rate) on catalysts coated RDE were measured in a O_2-satured 0.1 M KOH electrolyte at rotating rates from 100 to 1800 rpm. The numbers of electron transfer (n) were evaluated by Koutecky-Levich equation (3).

$$\frac{1}{i} = \frac{1}{i_k} + \left[\frac{1}{0.620nFAD^{2/3}\nu^{-1/6}C}\right]\omega^{-1/2} \quad (3)$$

Wherein, i is the measured current density, F is the Faraday constant (96485 C/mol), A is the electrode area (0.196 cm^2), D is the diffusion coefficient of the oxygen (1.93×10^{-5} cm^2 s^{-1}), ν is the kinematic viscosity of the solution (0.0109 cm^2 s^{-1}), C is the bulk concentration of oxygen (1.26×10^{-3} M), n is overall number of transferred number, ω is the angular rotation rate.

4. H_2O_2 measurements

To make a stock solution, 0.1 g of N,N-diethyl-1,4-phenylene-diamine sulfate (DPD, 97%, Aldrich) was dissolved in 10 mL of 0.1 N H_2SO_4 solution and 0.01 g of peroxidase (POD, horseradish, Aldrich) was dissolved in 10 mL of purified water. Buffer solution was prepared by mixing of 87.7 mL of 1 M monobasic sodium phosphate (Aldrich) solution, 12.6 mL of 1 M dibasic sodium phosphate heptahydrate (Aldrich) solution, and 99.7 mL of purified water. For

measurement, 0.4 mL of phosphate buffer, 1.12 mL of water, 1 mL of sample aliquots, 0.05 mL of DPD, and 0.05 mL of POD were mixed and kept under vigorous stirring for 90 seconds. The concentration of H_2O_2 was obtained by analyzing the absorbance at 551 nm using a Microplate Reader (Varioskan Lux, Thermo Scientific). [4]

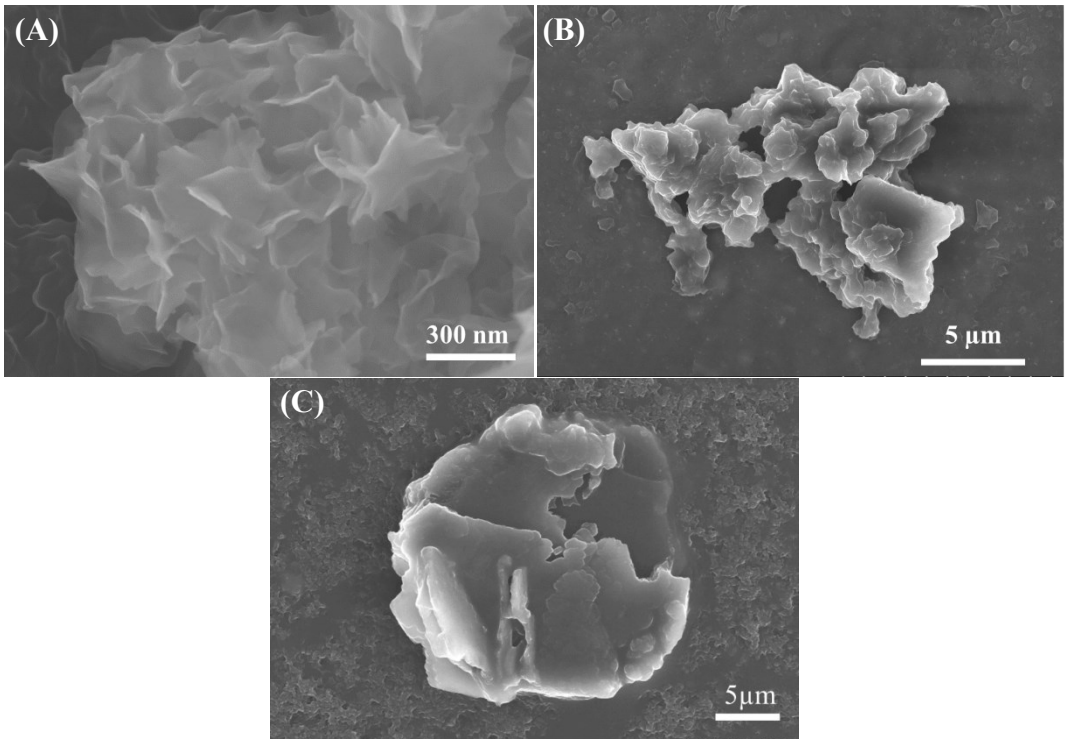

Figure S1. Typical scanning electron microscopy (SEM) images of (A) WSe_2 nanosheets; (B) pristine g-C_3N_4; and (C) bare g-C_3N_4 (BCN) synthesized by treating pristine g-C_3N_4 with $NaBH_4$.

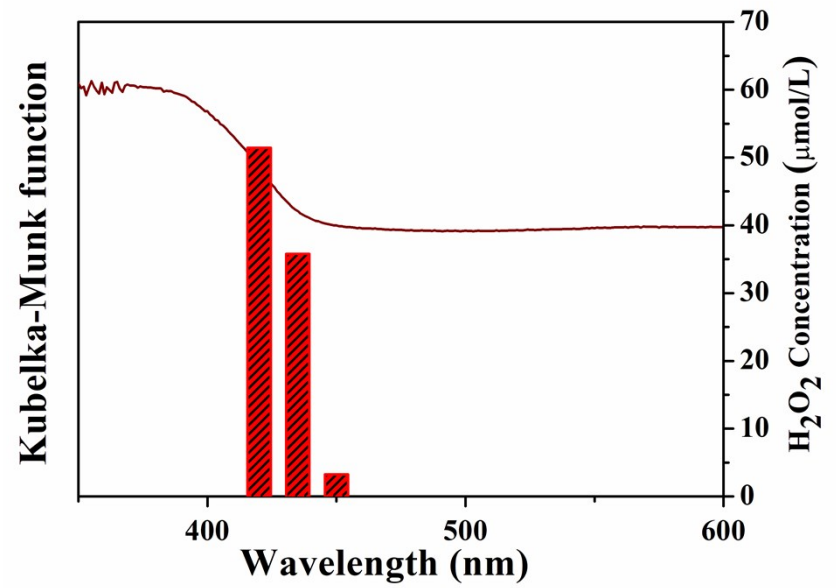

Figure S2. Wavelength dependent photocatalytic H_2O_2 evolution over WSe_2/g-C_3N_4 (CNW-4) under different monochromic light irradiation.

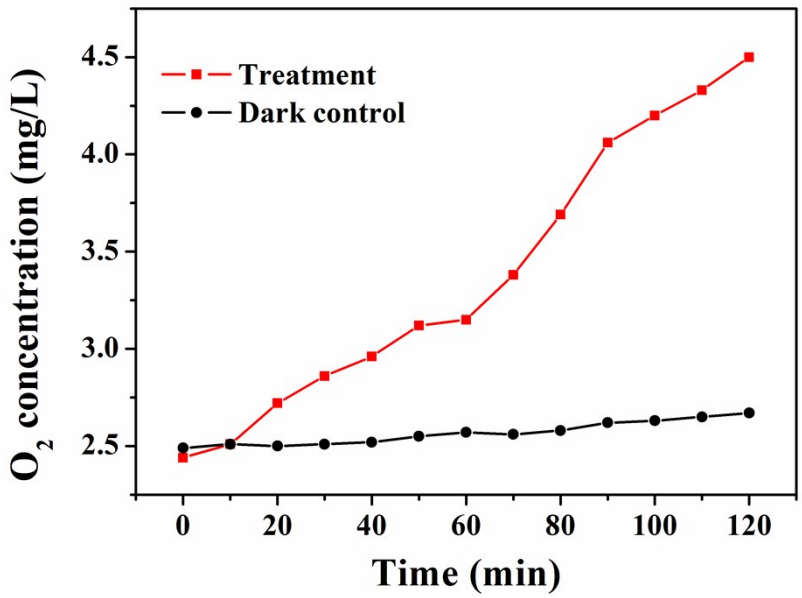

Figure S3. Time-dependent evolution of dissolved O_2 in the WSe_2/g-C_3N_4 (CNW-4) system under VL irradiation in a sealed reactor (pre-deoxygenated by N_2 bubbling for 0.5 h).

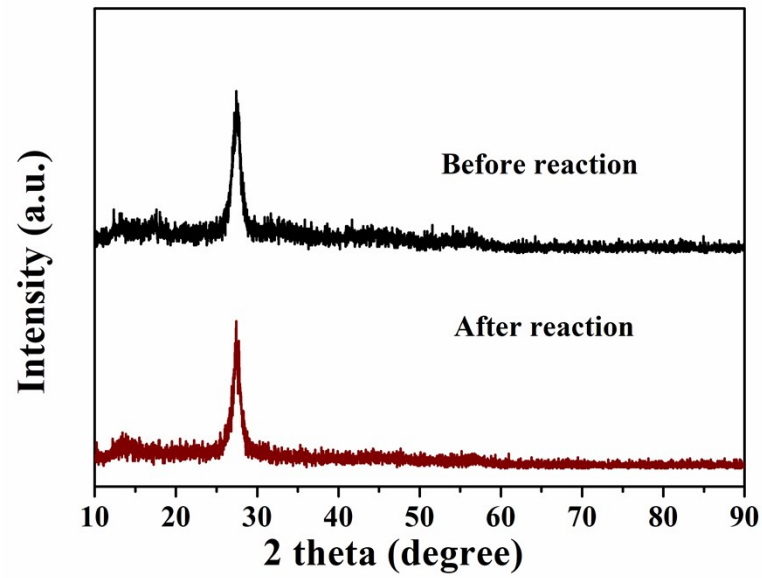

Figure S4. XRD pattern of CNW-4 before and after three successive repeated photocatalytic H_2O_2 production experiments

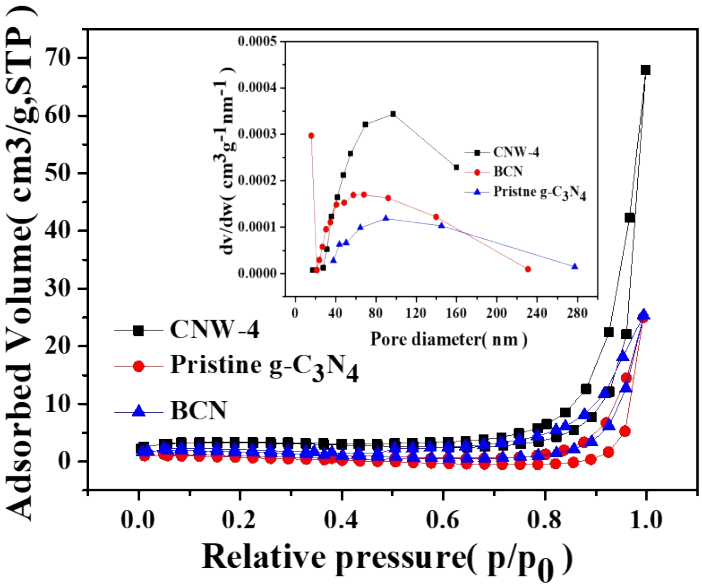

Figure S5. Nitrogen adsorption–desorption isotherms and the Barret–Joyner–Halenda (BJH) pore size distribution plot (inset) of the as-prepared pristine g-C_3N_4, bare g-C_3N_4 (BCN) and WSe_2/g-C_3N_4 (CNW-4).

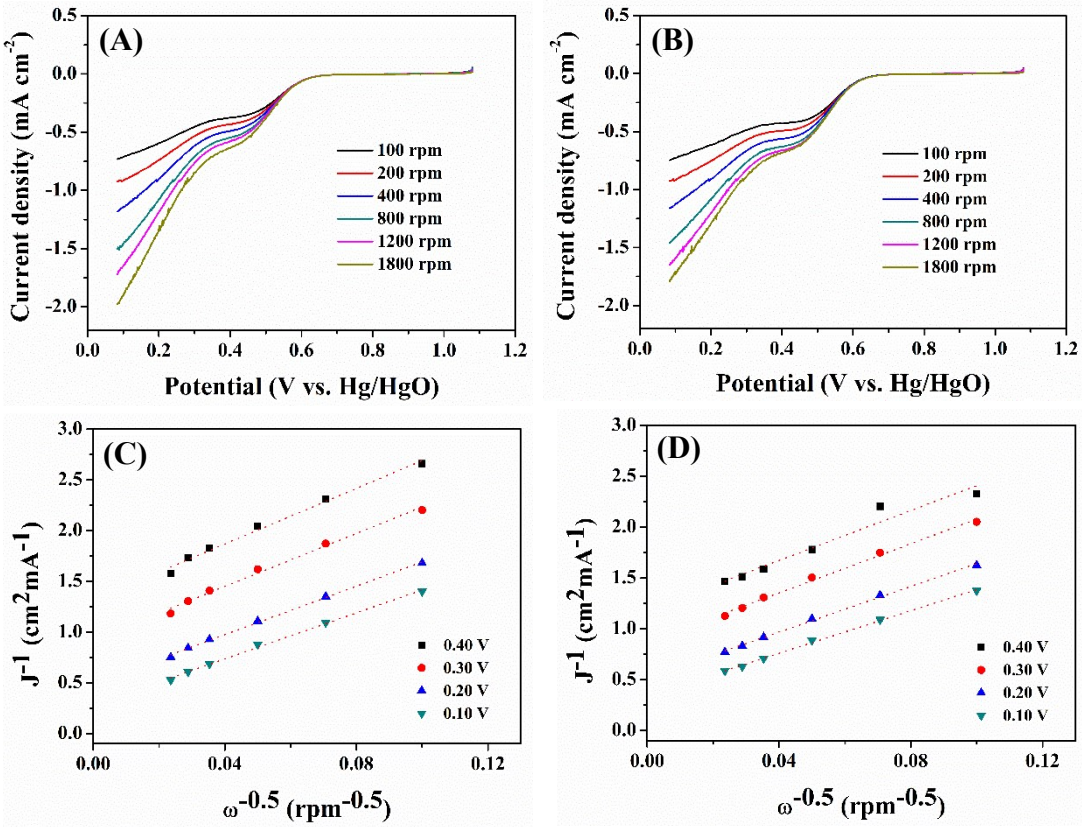

Figure S6. Linear sweep voltammetry (LSV) of (a) g-C_3N_4 and (b) CNW-4 at different rotation rates; Koutecky-Levich plots at different potentials for (a) g-C_3N_4 and (b) CNW-4.

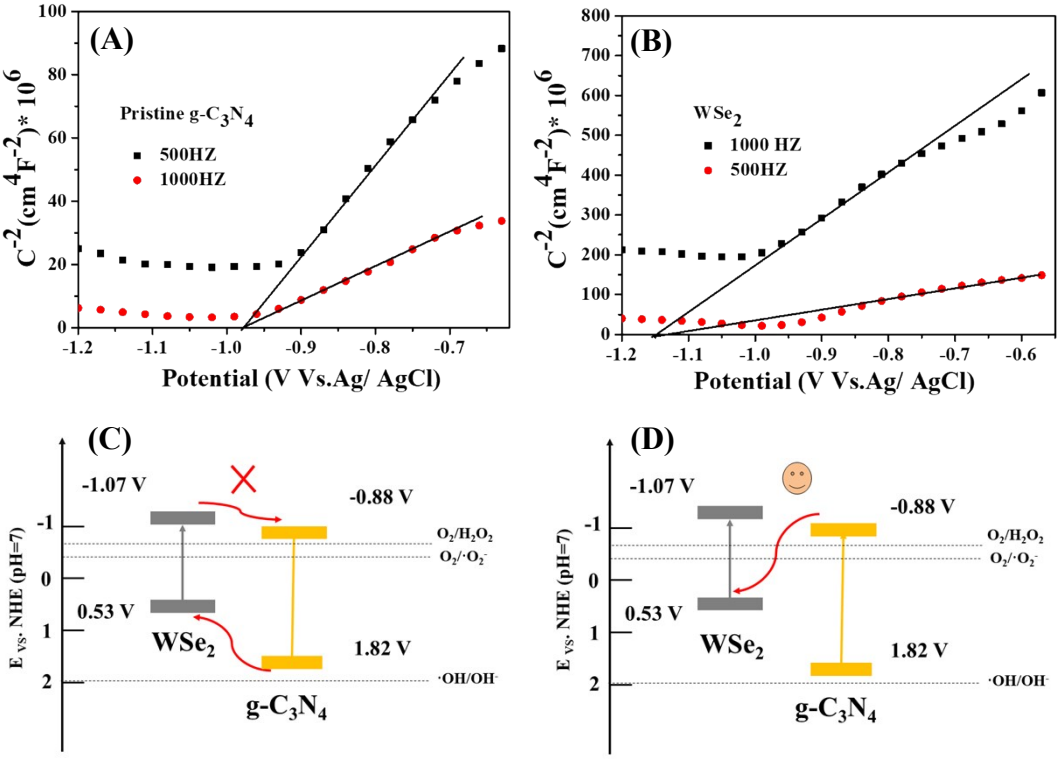

Figure S7. Mott–Schottky plots for (A) pristine g-C_3N_4 and (B) WSe_2 nanosheets with the frequency settled at 0.5 or 1.0 kHz; Schematic illustration of (C) Type II heterojunction charge transfer pathway and (D) Z-scheme pathway;

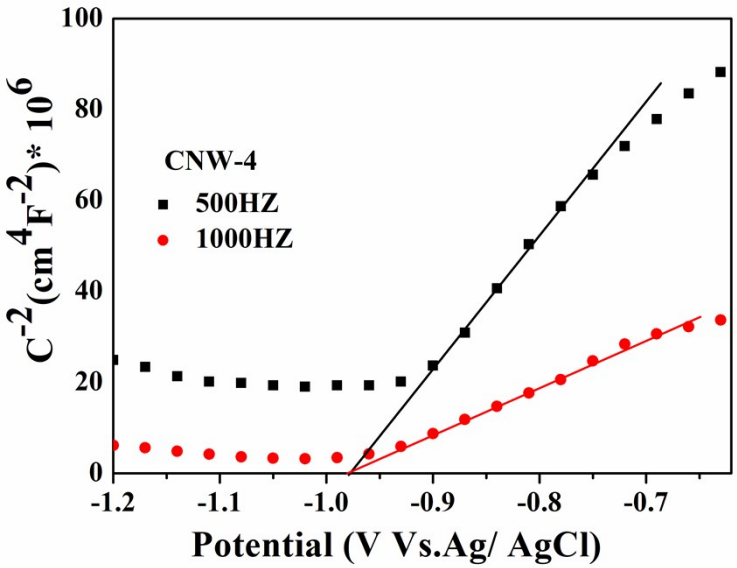

Figure S8. Mott–Schottky plots for WSe_2/g-C_3N_4 (CNW-4) composite showing similar flat-band potential (V_{fb}) as g-C_3N_4.

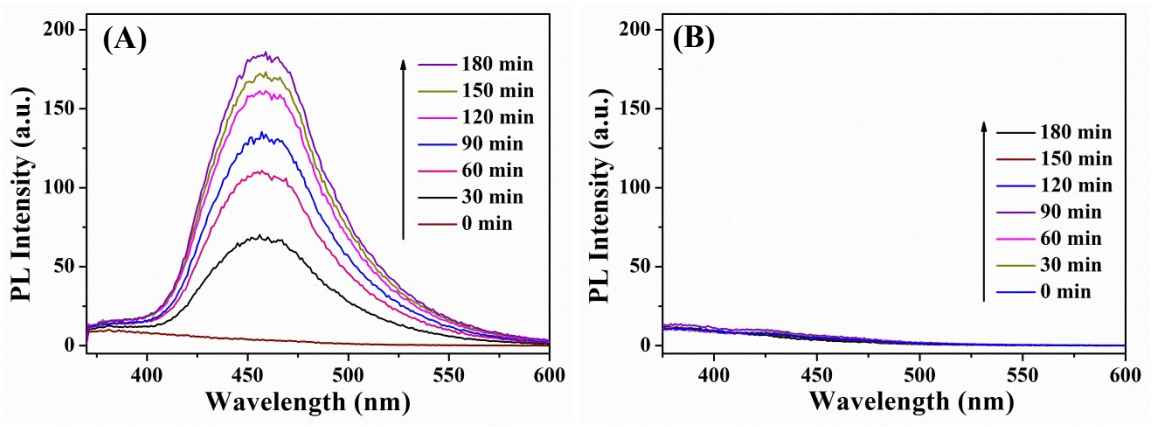

Figure S9. (A) Fluorescence spectra of coumarin solution (1 mM) in WSe_2/g-C_3N_4 (CNW-4) with Fe(II), and (B) without Fe (II) under VL irradiation.

Table S1. Comparison of photocatalytic production of H_2O_2 evolution in various representative works

Photocatalyst	**Photocatalyst concentration**	**Sacrificial agent**	**Light source**	**H_2O_2 amount** (μmol/L/h)	**Enhanced times compared with pristine g-C_3N_4**	**Reference**
Ti_3C_2/g-C_3N_4	1000 mg/L	10 % isopropanol	λ > 420 nm	132	2.1 times	[5]
[a] PT-g-C_3N_4	500 mg/L	10 % ethanol	λ > 400 nm	27.07	N.A.	[6]
[b] POM/g-C_3N_4	1000 mg/L	5 % methanol	AM 1.5	17.8	2.04 times	[7]
CNTs/g-C_3N_4	1000 mg/L	5% formic acid	λ > 400 nm	48.7	3.20 times	[8]
[c] BNQD/g-C_3N_4	1000 mg/L	10% IPA	λ > 420 nm	72.30	3.18 times	[9]
[d] BP /g-C_3N_4	1667 mg/L	10% IPA	λ > 420 nm	27	1.5 times	[10]
[a] PT-g-C_3N_4	500 mg/L	Pure water	λ > 400 nm	14.46	13 times	[6]
Inverse opal g-C_3N_4	1000 mg/L	Pure water	λ > 420 nm	23.12	2.36 times	[11]
CNTs/g-C_3N_4	1000 mg/L	Pure water	λ > 400 nm	13	5.2 times	[8]
[e] PI/g-C_3N_4	1000 mg/L	Pure water	λ > 420 nm	60	4.6 times	[12]
[b] POM/g-C_3N_4	1000 mg/L	Pure water	λ > 320 nm	35	2.69 times	[13]

g-C_3N_4 aerogels	1667 mg/L	Pure water	$\lambda > 420$ nm	48	3.86 times	[14]
WSe_2/g-C_3N_4 (CNW-4)	1000 mg/L	Pure water	$\lambda > 420$ nm	41	11.8 times	This work
	1000 mg/L	Ethanol	$\lambda > 420$ nm	120	35.0 times	This work

[a] Plasma-treated g-C_3N_4; [b] Polyoxometalates/g-C_3N_4; [c] Boron nitride quantum dots decorated g-C_3N_4; [d] Black phosphorus/g-C_3N_4; [e] perylene imides modified g-C_3N_4

References

1. B. Yu, B. J. Zheng, X. Q. Wang, F. Qi, J. R. He, W. L. Zhang and Y. F. Chen, Enhanced photocatalytic properties of graphene modified few-layered WSe_2 nanosheets, *Appl. Surf. Sci.*, 2017, **400**, 420-425.
2. X. Wang, J. He, B. Zheng, W. Zhang and Y. Chen, Few-layered WSe_2 in-situ grown on graphene nanosheets as efficient anode for lithium-ion batteries, *Electrochim. Acta*, 2018, **283**, 1660-1667.
3. S. L. Huang, H. Yi, L. H. Zhang, Z. Y. Jin, Y. J. Long, Y. Y. Zhang, Q. F. Liao, J. Na, H. Z. Cui, S. C. Ruan, Y. Yamauchi, T. Wakihara, Y. V. Kaneti and Y. J. Zeng, Non-precious molybdenum nanospheres as a novel cocatalyst for full-spectrum-driven photocatalytic CO_2 reforming to CH_4, *J. Hazard. Mater.*, 2020, **393**, 122324.
4. G.-H. Moon, D.-H. Kim, H.-I. Kim, A. D. Bokare and W. Choi, Platinum-like behavior of reduced graphene oxide as a cocatalyst on TiO_2 for the efficient photocatalytic oxidation of arsenite, *Environ. Sci. Technol. Lett.*, 2014, **1**, 185-190.
5. Y. Yang, Z. T. Zeng, G. M. Zeng, D. L. Huang, R. Xiao, C. Zhang, C. Y. Zhou, W. P. Xiong, W. J. Wang, M. Cheng, W. J. Xue, H. Guo, X. Tang and D. H. He, Ti_3C_2 Mxene/porous g-C_3N_4 interfacial Schottky junction for boosting spatial charge separation in photocatalytic H_2O_2 production, *Appl. Catal. B: Environ.*, 2019, **258**, 117956.
6. N. Lu, N. Liu, Y. Hui, K. Shang, N. Jiang, J. Li and Y. Wu, Characterization of highly effective plasma-treated g-C_3N_4 and application to the photocatalytic H_2O_2 production, *Chemosphere*, 2019, **241**, 124927.
7. S. Zhao, X. Zhao, S. X. Ouyang and Y. F. Zhu, Polyoxometalates covalently combined with graphitic carbon nitride for photocatalytic hydrogen peroxide production, *Catal. Sci. Technol.*, 2018, **8**, 1686-1695.
8. S. Zhao, T. Guo, X. Li, T. G. Xu, B. Yang and X. Zhao, Carbon nanotubes covalent combined with graphitic carbon nitride for photocatalytic hydrogen peroxide production under visible light, *Appl. Catal. B: Environ.*, 2018, **224**, 725-732.
9. Y. Yang, C. Zhang, D. L. Huang, G. M. Zeng, J. H. Huang, C. Lai, C. Y. Zhou, W. J. Wang, H. Guo, W. J. Xue, R. Deng, M. Cheng and W. P. Xiong, Boron nitride quantum dots decorated ultrathin porous g-C_3N_4: Intensified exciton dissociation and charge transfer for promoting visible-light-driven molecular oxygen activation, *Appl. Catal. B: Environ.*, 2019, **245**, 87-99.

10. Y. Zheng, Z. H. Yu, H. H. Ou, A. M. Asiri, Y. L. Chen and X. C. Wang, Black phosphorus and polymeric carbon nitride heterostructure for photoinduced molecular oxygen activation, *Adv. Funct. Mater.*, 2018, **28**, 1705407.
11. J. Y. Lei, B. Chen, W. J. Lv, L. Zhou, L. Z. Wang, Y. D. Liu and J. L. Zhang, Robust photocatalytic H_2O_2 production over inverse opal g-C_3N_4 with carbon vacancy under visible Light, *ACS Sustain. Chem. Eng.,* 2019, **7**, 16467-16473.
12. L. P. Yang, G. H. Dong, D. L. Jacobs, Y. H. Wang, L. Zang and C. Y. Wang, Two-channel photocatalytic production of H_2O_2 over g-C_3N_4 nanosheets modified with perylene imides, *J. Catal.*, 2017, **352**, 274-281.
13. S. Zhao, X. Zhao, H. Zhang, J. Li and Y. Zhu, Covalent combination of polyoxometalate and graphitic carbon nitride for light-driven hydrogen peroxide production, *Nano Energy*, 2017, **35**, 405-414.
14. H. H. Ou, P. J. Yang, L. H. Lin, M. Anpo and X. C. Wang, Carbon Nitride Aerogels for the Photoredox Conversion of Water, *Angew. Chem. Int. Edit.,* 2017, **56**, 10905-10910.